

Vibration-Based Structural Damage Detection and Precise Assessment via Stochastic Functionally Pooled Models

Fotis P. Kopsaftopoulos and Spilios D. Fassois

Stochastic Mechanical Systems & Automation (SMSA) Laboratory
Department of Mechanical & Aeronautical Engineering
University of Patras, GR 265 00 Patras, Greece
E-mail: {fkopsaf,fassois}@mech.upatras.gr

Keywords: damage localization, damage quantification, vibration based methods, stochastic methods

Abstract. This work aims at the precise assessment of a recently introduced method that, in addition to damage detection, allows for complete and accurate damage identification (localization) and magnitude estimation. The method is based on Vector-dependent Functionally Pooled (VFP) models and is capable of offering an effective and precise solution in a unified framework. The effectiveness of the method is experimentally assessed via its application to a prototype GARTEUR-type laboratory scale aircraft structure.

Introduction

The interest in the ability to monitor a structure and detect damage at an early stage is pervasive throughout the mechanical, aerospace and civil engineering communities. In fact, the combined problems of early detection, localization and magnitude estimation of damage are of paramount importance, as prompt detection may lead to better dynamic performance, increased safety and proper maintenance [1]. Vibration-based time series type methods for damage detection and assessment are among the most accurate and effective [1–4]. They offer a number of potential advantages, such as no requirement for visual inspection, “automation” capability, “global” coverage, and the ability to work at a “system level”. Nevertheless, and despite the fact that they generally tend to treat damage detection effectively, problems are frequently encountered when it comes to damage localization and magnitude estimation.

This work aims at the precise assessment of the recently introduced VFP-ARX model based method [5] that allows for complete and accurate damage localization and magnitude estimation. The method is based on novel *Vector-dependent Functionally Pooled AutoRegressive with exogenous excitation (VFP-ARX) models* [6], characterized by parameters that depend on damage magnitude and location, as well as proper statistical estimation and decision making schemes. The method is capable of offering an effective and precise solution to the damage detection, localization and magnitude estimation subproblems in a unified framework, accounting for experimental and measurement uncertainties and operating even on a single pair of measurements.

The Experimental Set-Up

The Structure. The scale aircraft structure considered was designed by ONERA in conjunction with the GARTEUR SM-AG19 Group and manufactured at the University of Patras (Fig. 1). It

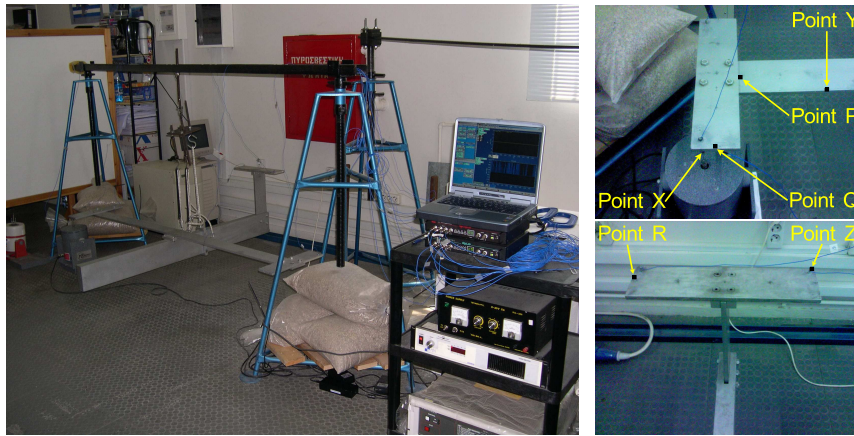


Figure 1. The aircraft skeleton structure and the experimental set-up: The force excitation (Point X) the vibration measurement positions (Points Y and Z), and the first damage location (Points P, Q and R) for the corresponding damage modes.

represents a typical aircraft design and consists of six solid beams with rectangular cross sections representing the fuselage ($1500 \times 150 \times 50$ mm), the wing ($2000 \times 100 \times 10$ mm), the horizontal ($300 \times 100 \times 10$ mm) and vertical stabilizers ($400 \times 100 \times 10$ mm), and the right and left wing tips ($400 \times 100 \times 10$ mm). All parts are constructed from standard aluminium and are jointed together via steel plates and screws. The total mass of the structure is approximately 50 kg.

The Damage. The damage considered corresponds to the attachment of a variable number of small masses, simulating local elasticity reductions, at three different sections (geometrical axes) of the structure. Each added mass weighs approximately 8.132 gr. The considered damage belongs to three distinct types (*damage/fault modes*) depending on the section of the structure they occur at.

The first type (*damage mode A*) corresponds to the attachment of up to 10 masses, covering the range of $[0, 81.32]$ gr (representing different damage magnitudes), at nine successive locations (at distances of 10 cm) starting from Point P (Fig. 1) and moving to the left along the right wing of the aircraft (Fig. 1). The complete series covers the range of $[0, 80]$ cm along the wing. The second type (*damage mode B*) corresponds to the attachment of masses ($[0, 81.32]$ gr) at five successive locations (at distances of 10 cm) starting from Point Q (Fig. 1) and moving backwards along the right wing-tip, with the complete series covering the range of $[0, 40]$ cm. The third type (*damage mode C*) corresponds to the attachment of masses ($[0, 81.32]$ gr) at five successive locations (at distances of 10 cm) starting from Point R (Fig. 1) and moving to the left along the horizontal stabilizer, with the complete series covering the range of $[0, 40]$ cm.

Each distinct damage is designated as F_{k^1, k^2}^X , with X indicating the damage mode, k^1 the specific damage magnitude (gr of added mass) and k^2 the exact damage location (distance in cm from Point P, Q or R). The healthy structure is designated as F_0 .

The Experiments. Damage detection, identification and magnitude estimation are based on vibration testing of the structure, which is suspended through a set of bungee cords under free-free boundary conditions.

The excitation is random stationary Gaussian force applied vertically at the right wing tip (Point X, Fig. 1) via an electromechanical shaker. The actual force exerted on the structure is measured via an impedance head, while the resulting vertical acceleration responses are measured at Points

Y and Z (Fig. 1) via lightweight (0.7 gr) accelerometers. The force and acceleration signals are driven through a conditioning charge amplifier into the data acquisition system.

A number of experiments for each damage mode is carried out, initially with the healthy structure and subsequently with the damaged, for each one of the mentioned damage locations and damage magnitudes. The acquired signals are digitized at 256 Hz (effective bandwidth 4-80 Hz), scaled and mean-corrected. Each resulting signal is $N = 1500$ samples long.

The VFP-ARX Model Based Method

The *Vector dependent Functionally Pooled ARX (VFP-ARX)* model based method [5] for combined damage detection, identification and magnitude estimation consists of two phases: (a) The *baseline phase*, which includes modelling of the damage modes considered (for the continuum of damage magnitudes and locations) via the novel class of stochastic VFP-ARX models. (b) The *inspection phase*, which is performed periodically or on demand during the structure's service cycle and includes the functions of damage detection, identification and magnitude estimation.

Baseline Phase. The modelling of the structure for a specific damage mode via a VFP-ARX model involves consideration of all admissible damage magnitudes occurring at predetermined locations on a specific section of the structure (right/left wing, horizontal stabilizer, and so on). For this reason a total of $M_1 \times M_2$ experiments is performed (physically or via simulation). Each experiment is characterized by a specific damage magnitude k^1 and a specific damage location k^2 , with the complete series covering the required range of each variable, say $[k_{min}^1, k_{max}^1]$ and $[k_{min}^2, k_{max}^2]$, via the discretizations $\{k_1^1, k_2^1, \dots, k_{M_1}^1\}$ and $\{k_1^2, k_2^2, \dots, k_{M_2}^2\}$.

A proper mathematical description of the structure for the considered damage mode may be obtained in the form of a VFP-ARX model. In the case of several vibration measurement locations, an array of such models may be obtained, with each scalar model corresponding to each measurement location.

The VFP-ARX(na, nb) model structure postulated is of the form¹ [6]:

$$y_{\mathbf{k}}[t] + \sum_{i=1}^{na} a_i(\mathbf{k}) \cdot y_{\mathbf{k}}[t-i] = \sum_{i=0}^{nb} b_i(\mathbf{k}) \cdot x_{\mathbf{k}}[t-i] + e_{\mathbf{k}}[t] \quad e_{\mathbf{k}}[t] \sim \text{NID}(0, \sigma_e^2(\mathbf{k})) \quad (1)$$

$$a_i(\mathbf{k}) \triangleq \sum_{j=1}^p a_{i,j} \cdot G_j(\mathbf{k}), \quad b_i(\mathbf{k}) \triangleq \sum_{j=1}^p b_{i,j} \cdot G_j(\mathbf{k}) \quad (2)$$

with na, nb designating the AutoRegressive (AR) and eXogenous (X) orders, respectively, $x_{\mathbf{k}}[t]$, $y_{\mathbf{k}}[t]$ the excitation and response signals, respectively, and $e_{\mathbf{k}}[t]$ the model's one-step-ahead prediction error (residual) sequence which is Normally Independently Distributed (NID) with zero mean and variance $\sigma_e^2(\mathbf{k})$. This sequence is potentially cross-correlated with its counterparts corresponding to different experiments.

As Eq. (2) indicates, the AR and X parameters $a_i(\mathbf{k})$, $b_i(\mathbf{k})$ are explicit functions of the vector \mathbf{k} by belonging to a p -dimensional functional subspace spanned by the (mutually independent) functions $G_1(\mathbf{k}), G_2(\mathbf{k}), \dots, G_p(\mathbf{k})$ (*functional basis*). The functional basis consists of polynomials of two variables (vector polynomials) obtained as tensor products from univariate polynomials

¹Lower case/capital bold face symbols designate vector/matrix quantities, respectively.

(Chebyshev or other families). The constants $a_{i,j}$, $b_{i,j}$ designate the AR and X, respectively, coefficients of projection.

The VFP-ARX model of Eqs. (1)-(2) is parameterized in terms of the parameter vector (to be estimated from the measured signals) $\bar{\theta} \triangleq [a_{i,j} : b_{i,j} : \sigma_e^2(\mathbf{k})]^T \forall \mathbf{k} \in \mathbb{R}^2$. The projection coefficient vector may be estimated via a Weighted Least Squares (WLS) criterion; see [6].

Inspection Phase. Let $x[t], y[t]$ ($t = 1, \dots, N$) represent the excitation and response signals, respectively, obtained from the structure in a *current* (unknown) state.

Damage detection may be based on the re-parameterized, in terms of \mathbf{k} and $\sigma_e^2(\mathbf{k})$, VFP-ARX model (keeping the projection coefficients at their previously estimated values) of *any* damage mode:

$$\mathcal{M}(\mathbf{k}, \sigma_e^2(\mathbf{k})) : y[t] + \sum_{i=1}^{na} a_i(\mathbf{k}) \cdot y[t-i] = \sum_{i=0}^{nb} b_i(\mathbf{k}) \cdot x[t-i] + e[t]. \quad (3)$$

The estimation of the unknown parameters $\mathbf{k}, \sigma_e^2(\mathbf{k})$ based on the current excitation – response signals, may be achieved via the following Nonlinear Least Squares (NLS) and variance estimators:

$$\hat{\mathbf{k}} \triangleq \arg \min_{\mathbf{k}} \sum_{t=1}^N e^2[t], \quad \sigma_e^2(\hat{\mathbf{k}}) = \frac{1}{N} \sum_{t=1}^N e^2[t, \hat{\mathbf{k}}] \quad (4)$$

the first one realized via a hybrid optimization scheme based on Genetic Algorithms and nonlinear optimization (sequential quadratic programming).

The first estimator may be shown to be asymptotically Gaussian distributed, with mean equal to the true \mathbf{k} value and covariance matrix $\Sigma_{\mathbf{k}}$ ($\hat{\mathbf{k}} \sim \mathcal{N}(\mathbf{k}, \Sigma_{\mathbf{k}})$) coinciding with the Cramer–Rao lower bound [6]. Since the healthy structure corresponds to $k^1 = 0$ (zero damage magnitude), damage detection may be based on a hypothesis testing problem solved via a t-test procedure [3].

Once damage occurrence has been detected, current damage mode determination is based on the successive estimation and validation of re-parameterized VFP-ARX models, each corresponding to each damage mode. The procedure stops as soon as a particular model is successfully validated, with the corresponding damage mode identified as the current one.

Damage identification (localization) and magnitude estimation are then based on the interval estimates of k^2 and k^1 , respectively, which are constructed based on the $\hat{\mathbf{k}}, \hat{\Sigma}_{\mathbf{k}}$ estimates obtained from the re-parameterized VFP-ARX model (of the form of Eq. (3)) of the *current* damage mode. Thus, the interval estimates of k^1 (damage magnitude) and k^2 (damage location) at the α risk level are [5]:

$$k^i \text{ interval estimate: } \left[\hat{k}^i + t_{\frac{\alpha}{2}}(N-2) \cdot \hat{\sigma}_{k^i}, \hat{k}^i + t_{1-\frac{\alpha}{2}}(N-2) \cdot \hat{\sigma}_{k^i} \right] \quad (5)$$

with $i = 1$ for damage magnitude and $i = 2$ for damage location, while $\hat{\sigma}_{k^i}$ is the positive square root of the i -th diagonal element of $\hat{\Sigma}_{\mathbf{k}}$.

Bivariate confidence bounds for $\mathbf{k} = [k^1 \ k^2]^T$ may be also obtained by observing that the quantity $(\hat{\mathbf{k}} - \mathbf{k})^T \Sigma_{\mathbf{k}}^{-1} (\hat{\mathbf{k}} - \mathbf{k})$ follows chi-square distribution with two degrees of freedom. Hence:

$$(\hat{\mathbf{k}} - \mathbf{k})^T \Sigma_{\mathbf{k}}^{-1} (\hat{\mathbf{k}} - \mathbf{k}) \leq \chi_{1-\alpha}^2(2) \quad \text{at the } \alpha \text{ risk level} \quad (6)$$

with $\chi_{1-\alpha}^2(2)$ designating the distribution's $1 - \alpha$ critical point. This expression defines an ellipsoid on the (k^1, k^2) plane within which the true (k^1, k^2) point should lie with probability $(1 - \alpha)$, or, equivalently, with risk α (*bivariate confidence bound*).

Experimental Results

Baseline Phase. Damage mode modelling for damage mode A (designated as $F_{\mathbf{k}}^A$), defined as the damage (attached masses) of all possible magnitudes at the right wing of the aircraft, is based on signals obtained from a total of $M_1 \times M_2 = 99$ experiments. 9 experiments correspond to the healthy structure ($k^1 = 0$ gr) and 90 to the various damaged structures (1–10 masses being placed at each one of the 9 locations on the right wing). The mass and location increments used are $\delta k^1 = 8.132$ gr and $\delta k^2 = 10$ cm, and the ranges of $[0, 81.32]$ gr and $[0, 80]$ cm are covered.

Damage mode modelling for damage modes B and C (designated as $F_{\mathbf{k}}^B$ and $F_{\mathbf{k}}^C$, respectively) is based on signals obtained from a total of $M_1 \times M_2 = 55$ experiments. 5 experiments correspond to the healthy structure ($k^1 = 0$ gr) and 50 to the damaged structure (1–10 masses being placed at each one of the 5 locations on the right wing-tip for fault mode B or on the horizontal stabilizer for fault mode C). The mass and location increments used are $\delta k^1 = 8.132$ gr and $\delta k^2 = 10$ cm, and the ranges of $[0, 81.32]$ gr and $[0, 40]$ cm are covered.

Three VFP-ARX damage mode models, based on excitation measurement point X and vibration measurement at points Y or Z (Fig. 1) are constructed. The VFP-ARX modelling procedure based on $N=1500$ sample-long excitation–response signals leads to a VFP-ARX(48, 48) model, with functional subspace consisting of $p = 30$ Chebyshev Type II vector polynomials, as the appropriate $F_{\mathbf{k}}^A$ damage mode model. Similarly, VFP-ARX(57, 57) and VFP-ARX(65, 65) models, with functional subspaces consisting of $p = 30$ Chebyshev Type II vector polynomials are selected as the appropriate $F_{\mathbf{k}}^B$ and $F_{\mathbf{k}}^C$ damage mode models, respectively.

Inspection Phase. Ten test cases, one corresponding to the healthy structure (F_0), seven to damage characterized by added masses attached to various locations on the right wing (damage mode A), right wing-tip (damage mode B) and horizontal stabilizer (damage mode C), not necessarily coinciding with those used in the baseline phase, and two test cases corresponding to unmodelled damage (not belonging to any modelled damage mode – 40 gr attached to the left wing and wing-tip, respectively) are considered. The corresponding damage mode identification results are pictorially presented in Fig. 2, while the damage detection, localization and magnitude estimation results are presented in Fig. 3.

In the first case of Fig. 3 (healthy structure, F_0) the interval estimate of only the damage magnitude (gr) is meaningful. Evidently, no damage is detected as the interval estimate at the $\alpha = 0.05$ risk level (shaded strip) includes the $k^1 = 0$ value (notice that the dashed vertical line designates the true damage magnitude, while the middle line the point estimate and the left and right vertical lines the lower and upper confidence bounds, respectively). In the rest of the cases the bivariate (k^1, k^2) confidence bounds (at the $\alpha = 0.05$ risk level) are depicted. Damage is, in each of these cases, rightly detected as the damage magnitude's interval estimate does not include the $k^1 = 0$ value (vertical axis). It should be further observed that very accurate estimates of the damage magnitude and location, characterized by narrow confidence bounds, are obtained.

Acknowledgement

The authors thank the European Social Fund (ESF), Operational Program for Educational and Vocational Training II (EPEAEK II), and particularly the Program PYTHAGORAS, for funding this work.

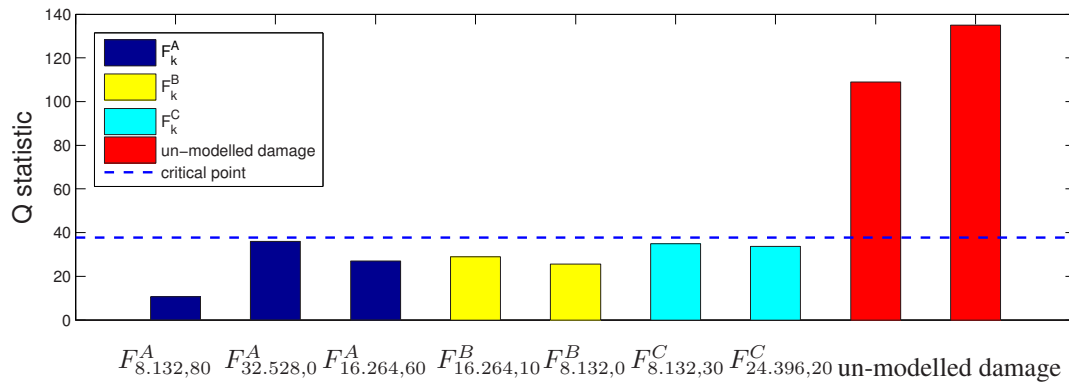


Figure 2. Damage identification results: Q statistic (bars) and the critical point (---) at the $\alpha = 0.05$ level ($h = 25$). The considered damage mode is identified as current if Q is lower than the critical point.

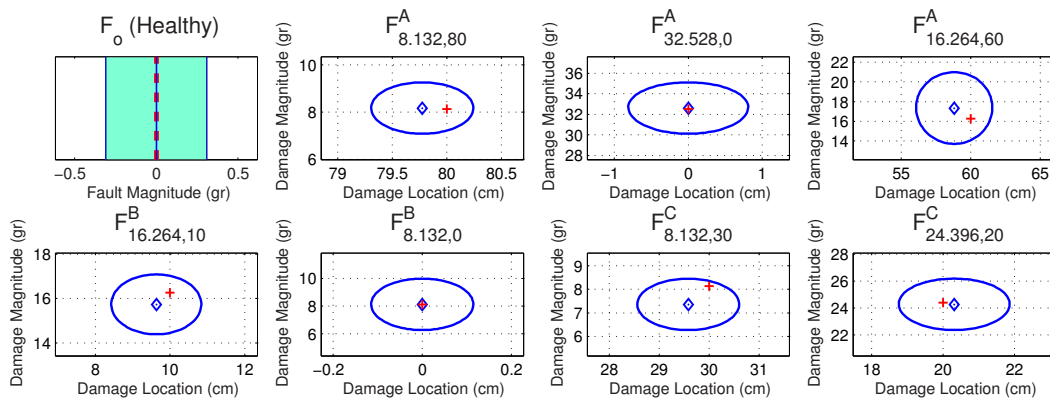


Figure 3. Damage detection, localization and magnitude estimation results for six test cases (the correct damage indicated above the plot; for the first test case the confidence bound of only the damage magnitude is meaningful; for the other test cases the bivariate confidence bounds are depicted at the $\alpha = 0.05$ risk level [+ : true values, \diamond : point estimates]).

References

- [1] S.W. Doebling, C.R. Farrar, M.B. Prime and D.W. Shevitz: Report LA-13070-MS, Los Alamos National Laboratory, USA (1996).
- [2] Y. Zou, L. Tong, and G.P. Steven: Journal of Sound and Vibration Vol. 230 (2000), p. 357.
- [3] S.D. Fassois and J.S. Sakellariou: Philosophical Transactions of the Royal Society A: Mathematical, Physical and Engineering Sciences Vol. 365 (2007), p. 411.
- [4] M. Basseville, M. Abdelghani and A. Benveniste: Automatica Vol. 36 (2000), p. 101.
- [5] F.P. Kopsaftopoulos and S.D. Fassois, in: *Proc. of the 3rd European Workshop on Structural Health Monitoring*, Granada, Spain (2006).
- [6] F.P. Kopsaftopoulos and S.D. Fassois, in: *Proc. of the Mediterranean Conference on Control and Automation*, Ancona, Italy (2006).